

# STATIC ANALYSIS OF REISSNER-MINDLIN PLATES USING ES+NS-MITC3 ELEMENTS

Chau Dinh Thanh<sup>a,\*</sup>, Ho Thi Con<sup>b</sup>, Le Phuong Binh<sup>a</sup>

<sup>a</sup>*Faculty of Civil Engineering, HCMC University of Technology and Education,  
1 Vo Van Ngan street, Thu Duc district, Ho Chi Minh city, Vietnam*

<sup>b</sup>*Center for Vocational and Regular Education, Chau Phu district, An Giang province, Vietnam*

## **Article history:**

*Received 09/08/2019, Revised 29/08/2019, Accepted 30/08/2019*

---

## **Abstract**

In this research, the smoothed finite element methods (S-FEM) based on the edge-based (ES) and node-based (NS) approaches are combined to develop for the 3-node triangular plate element which uses the mixed interpolation of tensorial components (MITC3) technique to remove the shear-locking phenomenon. This approach is based on the  $\beta$ FEM in which the parameter  $\beta$  is used to tune the contribution ratio of the edge-based and node-based smoothed domains. The strain fields of the proposed ES+NS-MITC3 element are smoothed on a part of the edge-based domains and the other on the node-based domains which are respectively defined by elements sharing common edges and common nodes. The ES+NS-MITC3 element passes the patch test and is employed to statically analyze some benchmark Reissner-Mindlin plates, including square and rhombus ones. Numerical results show that, in both thin and thick plates the ES+NS-MITC3 element can give results better than similar elements using the ES-FEM or NS-FEM only.

*Keywords:* Reissner-Mindlin plates; MITC3; ES-FEM; NS-FEM.

[https://doi.org/10.31814/stce.nuce2019-13\(3\)-05](https://doi.org/10.31814/stce.nuce2019-13(3)-05) © 2019 National University of Civil Engineering

---

## **1. Introduction**

Plate is one of the most popular structures in construction, shipbuilding, automotive or aerospace industries due to its advantages of load-carrying capacity and aesthetics. Instead of using analytical approaches [1–3], to determine the behaviors of complex plate structures the finite element methods (FEM) are widely employed. Then many plate finite elements have been developed, especially triangular elements based on the thick plate theory of Reissner-Mindlin which includes the transverse shear strains [1]. One of the simplest triangular elements is the 3-node triangular element because it uses the  $C^0$ -type displacement approximation and is most efficient to discretize arbitrary plate geometries. However, the original  $C^0$ -type elements always exists non-zero transverse shear strains and leads to underestimate the deflection, or the shear-locking phenomenon, of the thin plates which ignore the transverse shear strains according to the Kirchhoff-Love plate theory. To make the  $C^0$ -type elements be used for analysis of both thin and thick plates, various techniques have been suggested and successfully applied to alleviate the shear locking. The Mindlin-type 3 node (MIN3) [4], the discrete shear gap (DSG3) [5], or the mixed interpolation of tensorial components (MITC3) [6] techniques are some of efficient approaches to attenuate the shear locking in the 3-node triangular element. Especially, the

---

\*Corresponding author. *E-mail address:* [chdthanh@hcmute.edu.vn](mailto:chdthanh@hcmute.edu.vn) (Thanh, C. D.)

MITC3 approach satisfies the requirement of spatial isotropy, meaning that the element stiffness matrices are independent of the sequence of node numbering. Consequently, the plate elements MIN3, DSG3 or MITC3 can be used to analyze both thin and thick Reissner-Mindlin plates.

The strain fields of the 3-node triangular elements are constant on element domains because of  $C^0$ -type displacement approximation. To reduce much difference in strain fields between the elements, the smoothed finite element methods (SFEM) have been proposed [7]. According to the SFEM, the strain fields can be averaged over smoothed domains defined by adjacent elements having common edges or common nodes, namely the edge-based smoothed (ES) or the node-based smoothed (NS) methods respectively. Although the cell-based smoothed (CS) method is the other type of the SFEM, it is identical to the FEM when applied for the isotropic 3-node triangular elements. The ES- and NS-FEM have been successfully developed for the DSG3 and MITC3 plate elements [8–11].

Numerical results show that the ES-FEM usually brings overly stiff effects on the behaviors of the discretized model. In contrast, the NS-FEM causes overly soft behaviors in comparison with analytical solutions. To narrow the gap in results provided by the SFEM and the analytical solutions, the hybrid SFEM or  $\beta$ FEM has been suggested [12, 13] by reconstructing a new smoothed strain fields which includes the ES- and NS-strain fields. In this approach, a scale factor  $\beta \in [0,1]$  is used to tune the contribution ratio of ES- and NS-domains into the hybrid smoothed strain fields. The  $\beta$ FEM for the DSG3 plate element has demonstrated the superior performance when analyzing statics and vibration of the Reissner-Mindlin plates [12, 13]. Therefore, the  $\beta$ FEM will be developed for the MITC3 triangular plate element in this work. The proposed plate element, called ES+NS-MITC3 element, will be studied the accuracy and efficiency in the static analysis of the Reissner-Mindlin plates.

The paper is organized as follows. In the next section, the finite element formulae of the MITC3, ES-MITC3, NS-MITC3 elements are briefly reviews and then the development of the ES+NS-MITC3 element is presented. The numerical performance of the ES+NS-MITC3 element is evaluated through the static analyses of some benchmark plate problems in Section 3. In the last section, significant conclusions about the proposed element are withdrawn.

## 2. Finite element formulation of ES+NS-MITC3 based on the Reissner-Mindlin plate theory

### 2.1. MITC3 plate element

Consider a bending plate with the mid-surface of area  $A$  as shown in Fig. 1. The plate is subjected to loadings  $q$  normal to the mid-surface. According to the Reissner-Mindlin thick plate theory, the translational displacements  $u, v, w$  related to the  $x, y, z$ -directions are determined by [1]

$$u(x, y, z) = z\beta_x(x, y); \quad v(x, y, z) = z\beta_y(x, y); \quad w(x, y, z) = w_0(x, y) \quad (1)$$

where  $w_0, \beta_x, \beta_y$  are respectively the deflection and the rotations of the mid-surface about  $y$ - and  $x$ -axis with positive directions as shown in Fig. 1.

The mid-surface is discretized by the 3-node triangular elements. The displacements of the mid-surface are approximated by [14]

$$w_0 = \sum_{i=1}^3 N_i w_i; \quad \beta_x = \sum_{i=1}^3 N_i \theta_{yi}; \quad \beta_y = - \sum_{i=1}^3 N_i \theta_{xi} \quad (2)$$

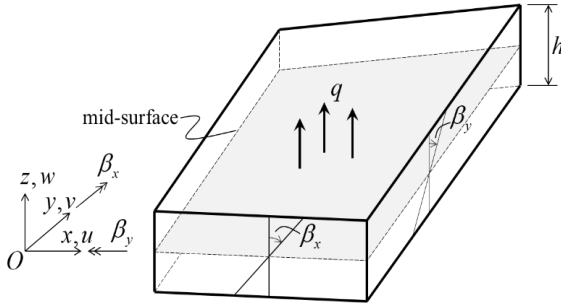


Figure 1. Definition of loadings and the positive displacements of the mid-surface of the Reissner-Mindlin plate

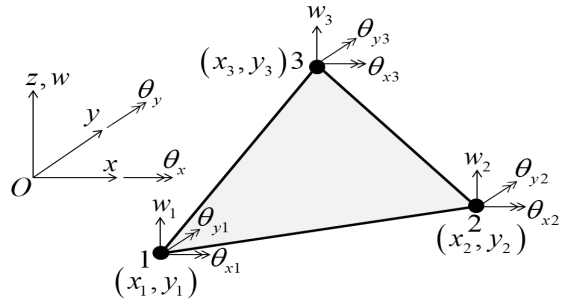


Figure 2. The 3-node triangular plate element and its positive directions of the nodal displacements

in which  $w_i, \theta_{xi}, \theta_{yi}$  are respectively the deflection and rotations of node  $i$  with the positive directions defined in Fig. 2; and the shape functions are

$$\begin{aligned} N_1 &= \frac{1}{2A_e} [(x_2y_3 - x_3y_2) + (y_2 - y_3)x + (x_3 - x_2)y] \\ N_2 &= \frac{1}{2A_e} [(x_3y_1 - x_1y_3) + (y_3 - y_1)x + (x_1 - x_3)y] \\ N_3 &= \frac{1}{2A_e} [(x_1y_2 - x_2y_1) + (y_1 - y_2)x + (x_2 - x_1)y] \end{aligned} \quad (3)$$

where  $x_i, y_i$  are the nodal coordinates of node  $i$  as shown in Fig. 2; and  $A_e$  is the area of the element.

From Eqs. (1) and (2), the relationships between the strains and the nodal displacements are determined

$$\begin{Bmatrix} \varepsilon_x \\ \varepsilon_y \\ \gamma_{xy} \end{Bmatrix} = z \begin{Bmatrix} \partial\beta_x/\partial x \\ \partial\beta_y/\partial y \\ \partial\beta_x/\partial y + \partial\beta_y/\partial x \end{Bmatrix} = z \sum_{i=1}^3 \underbrace{\begin{bmatrix} 0 & 0 & N_{i,x} \\ 0 & -N_{i,y} & 0 \\ 0 & -N_{i,x} & N_{i,y} \end{bmatrix}}_{\mathbf{B}_{bi}} \underbrace{\begin{Bmatrix} w_i \\ \theta_{xi} \\ \theta_{yi} \end{Bmatrix}}_{\mathbf{d}_{ei}} = z \sum_{i=1}^3 \mathbf{B}_{bi} \mathbf{d}_{ei} \quad (4)$$

$$\begin{Bmatrix} \gamma_{xz} \\ \gamma_{yz} \end{Bmatrix} = \begin{Bmatrix} \beta_x + \partial w_0/\partial x \\ \beta_y + \partial w_0/\partial y \end{Bmatrix} = \sum_{i=1}^3 \underbrace{\begin{bmatrix} N_{i,x} & 0 & N_i \\ N_{i,x} & -N_i & 0 \end{bmatrix}}_{\mathbf{B}_{si}} \underbrace{\begin{Bmatrix} w_i \\ \theta_{xi} \\ \theta_{yi} \end{Bmatrix}}_{\mathbf{d}_{ei}} = \sum_{i=1}^3 \mathbf{B}_{si} \mathbf{d}_{ei} \quad (5)$$

where the gradients  $\mathbf{B}_{bi}$  of the in-plane strains are given by

$$\mathbf{B}_{b1} = \frac{1}{2A_e} \begin{bmatrix} 0 & 0 & b-c \\ 0 & a-d & 0 \\ 0 & c-b & d-a \end{bmatrix}; \quad \mathbf{B}_{b2} = \frac{1}{2A_e} \begin{bmatrix} 0 & 0 & c \\ 0 & d & 0 \\ 0 & -c & -d \end{bmatrix}; \quad \mathbf{B}_{b3} = \frac{1}{2A_e} \begin{bmatrix} 0 & 0 & -b \\ 0 & -a & 0 \\ 0 & b & a \end{bmatrix} \quad (6)$$

in which  $a = x_2 - x_1, b = y_2 - y_1, c = y_3 - y_1, d = x_3 - x_1$ .

With the approximation of the transverse shear strains given by Eq. (5), there is always existence of the transverse shear strains in analyzed plates. In other words, the pure 3-node triangular element cannot be used for analysis of thin plates in which there are not the transverse shear strains according

to the Kirchhoff-Love thin plate theory. To be employed for both thin and thick plates, from the mixed interpolation of tensorial components approach the transverse shear strains in Eq. (5) are re-interpolated to be linear variations corresponding to the three edge directions of the element but be constant on the edges. The interpolations of the transverse shear strains connect the displacement approximations at tying points located at the mid-edges. The assumed transverse shear strains have been designed by Lee and Bathe [6] for the continuum mechanics based 3-node triangular shell finite elements, namely MITC3 technique to remove the shear locking. As a result, the transverse shear strains in Eq. (5) can be rewritten as

$$\begin{Bmatrix} \gamma_{xz}^{MITC3} \\ \gamma_{yz}^{MITC3} \end{Bmatrix} = \sum_{i=1}^3 \mathbf{B}_{si}^{MITC3} \mathbf{d}_{ei} \quad (7)$$

in which by using one Gaussian quadrature point located at the centroid of the element,  $\mathbf{B}_{si}^{MITC3}$  have been derived by Chau-Dinh et al. [10] in the explicit formulation, which only depends on nodal coordinates, as follows

$$\begin{aligned} \mathbf{B}_{s1}^{MITC3} &= \frac{1}{2A_e} \begin{bmatrix} b-c & (b-c)(b+c)/6 & A_e + (d-a)(b+c)/6 \\ d-a & -A_e - (b-c)(a+d)/6 & -(d-a)(a+d)/6 \end{bmatrix} \\ \mathbf{B}_{s2}^{MITC3} &= \frac{1}{2A_e} \begin{bmatrix} c & -bc/2 + c(b+c)/6 & ac/2 - d(b+c)/6 \\ -d & bd/2 - c(a+d)/6 & -ad/2 + d(a+d)/6 \end{bmatrix} \\ \mathbf{B}_{s3}^{MITC3} &= \frac{1}{2A_e} \begin{bmatrix} -b & -bc/2 - b(b+c)/6 & -bd/2 + a(b+c)/6 \\ a & -ac/2 + b(a+d)/6 & ad/2 - a(a+d)/6 \end{bmatrix} \end{aligned} \quad (8)$$

The constitutive relations between the stresses and the strains in the isotropic linear plates give

$$\begin{Bmatrix} \sigma_x \\ \sigma_y \\ \tau_{xy} \end{Bmatrix} = \frac{E}{1-\nu^2} \begin{bmatrix} 1 & \nu & 0 \\ \nu & 1 & 0 \\ 0 & 0 & (1-\nu)/2 \end{bmatrix} \begin{Bmatrix} \varepsilon_x \\ \varepsilon_y \\ \gamma_{xy} \end{Bmatrix} = \frac{Ez}{1-\nu^2} \begin{bmatrix} 1 & \nu & 0 \\ \nu & 1 & 0 \\ 0 & 0 & (1-\nu)/2 \end{bmatrix} \sum_{i=1}^3 \mathbf{B}_{bi} \mathbf{d}_{ei} \quad (9)$$

$$\begin{Bmatrix} \tau_{xz} \\ \tau_{yz} \end{Bmatrix} = \frac{E}{2(1-\nu)} \begin{Bmatrix} \gamma_{xz}^{MITC3} \\ \gamma_{yz}^{MITC3} \end{Bmatrix} = \frac{E}{2(1-\nu)} \sum_{i=1}^3 \mathbf{B}_{si}^{MITC3} \mathbf{d}_{ei} \quad (10)$$

with the Young's modulus  $E$  and the Poisson's ratio  $\nu$ .

The total potential energy of the plate subjected to the normal loadings  $q$  is expressed in matrix notation as [14]

$$\Pi = \int_A \int_{-h/2}^{h/2} \frac{1}{2} [\varepsilon_x \varepsilon_y \gamma_{xy}] \begin{Bmatrix} \sigma_x \\ \sigma_y \\ \tau_{xy} \end{Bmatrix} dz dA + \frac{kh^2}{h^2 + \alpha h_e^2} \int_A \int_{-h/2}^{h/2} \frac{1}{2} [\gamma_{xz}^{MITC3} \gamma_{yz}^{MITC3}] \begin{Bmatrix} \tau_{xz} \\ \tau_{yz} \end{Bmatrix} dz dA - \int_A w q dA = 0 \quad (11)$$

where the shear correction  $k$  is 5/6; the stabilized factor  $\alpha$  is 0.1; and  $h_e$  is the maximum length of the element's edges [15].

Using Eqs. (4), (7), (9), and (10), the total potential energy is written by

$$\Pi = \sum_{e=1}^{N_e} \frac{1}{2} \mathbf{d}_e^T \left( \int_{A_e} \mathbf{B}_b^T \mathbf{D}_b \mathbf{B}_b dA \right) \mathbf{d}_e + \sum_{e=1}^{N_e} \frac{1}{2} \mathbf{d}_e^T \left( \int_{A_e} (\mathbf{B}_s^{MITC3})^T \mathbf{D}_s \mathbf{B}_s^{MITC3} dA \right) \mathbf{d}_e - \sum_{e=1}^{N_e} \mathbf{d}_e^T \int_{A_e} \mathbf{N} q dA = 0 \quad (12)$$

in which  $\mathbf{B}_b = [\mathbf{B}_{b1} \ \mathbf{B}_{b2} \ \mathbf{B}_{b3}]$ ;  $\mathbf{B}_s^{MITC3} = [\mathbf{B}_{s1}^{MITC3} \ \mathbf{B}_{s2}^{MITC3} \ \mathbf{B}_{s3}^{MITC3}]$ ;  $\mathbf{d}_e = [\mathbf{d}_{e1}^T \ \mathbf{d}_{e2}^T \ \mathbf{d}_{e3}^T]^T$ ;  $\mathbf{N} = [N_1 \ 0 \ 0 \ N_2 \ 0 \ 0 \ N_3 \ 0 \ 0]^T$  and

$$\mathbf{D}_b = D \begin{bmatrix} 1 & \nu & 0 \\ \nu & 1 & 0 \\ 0 & 0 & (1-\nu)/2 \end{bmatrix} \quad \text{with } D = \frac{Eh^3}{12(1-\nu^2)} \quad (13)$$

$$\mathbf{D}_s = \frac{kEh^3}{(h^2 + \alpha h_e^2)2(1+\nu)} \begin{bmatrix} 1 & 0 \\ 0 & 1 \end{bmatrix} \quad (14)$$

Differentiating  $\Pi$  in Eq. (12) with respect to  $\mathbf{d}_e$  and equating each term to zero to minimize  $\Pi$ , the discretized equilibrium equations are obtained as follows

$$\mathbf{Kd} = \mathbf{F} \quad (15)$$

where  $\mathbf{d}$  is the nodal displacements of the plate;  $\mathbf{K}$  is the global stiffness matrix and assembled from the element stiffness matrices

$$\begin{aligned} \mathbf{k}_e &= \int_{A_e} \mathbf{B}_b^T \mathbf{D}_b \mathbf{B}_b dA + \int_{A_e} (\mathbf{B}_s^{MITC3})^T \mathbf{D}_s \mathbf{B}_s^{MITC3} dA \\ &= \mathbf{B}_b^T \mathbf{D}_b \mathbf{B}_b A_e + (\mathbf{B}_s^{MITC3})^T \mathbf{D}_s \mathbf{B}_s^{MITC3} A_e \end{aligned} \quad (16)$$

and  $\mathbf{F}$  is the global load vector and assembled from the element load vectors

$$\mathbf{f}_e = \int_{A_e} \mathbf{N} q dA \quad (17)$$

### 2.2. ES-MITC3 plate element

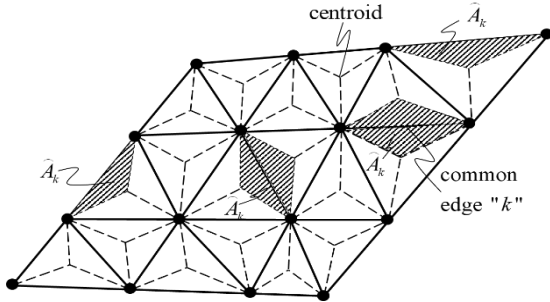


Figure 3. Edge-based smoothed domains for a plate discretized by 3-node elements

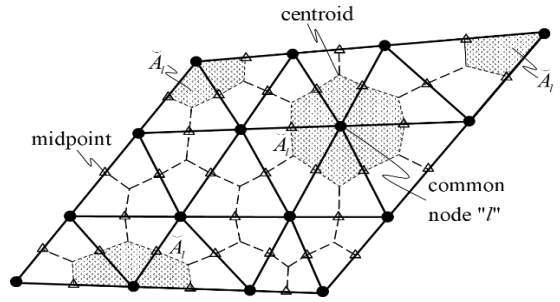


Figure 4. Node-based smoothed domains for a plate discretized by 3-node elements

In the edge-based smoothed FEM [7], strain fields are averaged on domains of two adjacent elements. Particularly, the edge-based smoothed domains are defined by straight lines which connect the edge's nodes with the centroids of two elements sharing this edge as shown in Fig. 3. Therefore, the ES-MITC3 plate element [10] is the MITC3 one in which the strain fields given by Eqs. (9) and (10) are smoothed as follows

$$\left\{ \begin{matrix} \widehat{\varepsilon}_x \\ \widehat{\varepsilon}_y \\ \widehat{\gamma}_{xy} \end{matrix} \right\} = \frac{1}{\widehat{A}_k} \int_{\widehat{A}_k} \left\{ \begin{matrix} \varepsilon_x \\ \varepsilon_y \\ \gamma_{xy} \end{matrix} \right\} dA; \quad \left\{ \begin{matrix} \widehat{\tau}_{xz} \\ \widehat{\tau}_{yz} \end{matrix} \right\} = \frac{1}{\widehat{A}_k} \int_{\widehat{A}_k} \left\{ \begin{matrix} \tau_{xz} \\ \tau_{yz} \end{matrix} \right\} dA \quad (18)$$

where  $\widehat{A}_k$  is the edge-based smoothed domain of edge “ $k$ ”.

Using the relationships between the strain fields and nodal displacements given by Eqs. (9) and (10), the smoothed strains fields in Eq. (18) can be expressed

$$\begin{Bmatrix} \widehat{\varepsilon}_x \\ \widehat{\varepsilon}_y \\ \widehat{\gamma}_{xy} \end{Bmatrix} = \frac{Ez}{1-\nu^2} \begin{bmatrix} 1 & \nu & 0 \\ \nu & 1 & 0 \\ 0 & 0 & (1-\nu)/2 \end{bmatrix} \underbrace{\left[ \frac{1}{\widehat{A}_k} \sum_{e=1}^{\widehat{N}_e} \left( \frac{A_e}{3} \sum_{i=1}^3 \mathbf{B}_{bi}^e \mathbf{d}_{ei} \right) \right]}_{\widehat{\mathbf{B}}_b \mathbf{d}^k} \quad (19)$$

$$\begin{Bmatrix} \widehat{\tau}_{xz} \\ \widehat{\tau}_{yz} \end{Bmatrix} = \frac{E}{2(1-\nu)} \underbrace{\left[ \frac{1}{\widehat{A}_k} \sum_{e=1}^{\widehat{N}_e} \left( \frac{A_e}{3} \sum_{i=1}^3 \mathbf{B}_{si}^{MITC3,e} \mathbf{d}_{ei} \right) \right]}_{\widehat{\mathbf{B}}_s \mathbf{d}^k} \quad (20)$$

in which  $\widehat{A}_k$  is the area of edge-based smoothed domain “ $k$ ”;  $\widehat{N}_e = 1$  for edge “ $k$ ” on the boundary and  $\widehat{N}_e = 2$  for the others;  $\widehat{\mathbf{B}}_b, \widehat{\mathbf{B}}_s$  are respectively the gradient matrices of the in-plane and transverse shear smoothed strains; and  $\mathbf{d}^k$  is the nodal displacements related to the smoothed domain “ $k$ ”.

Substituting Eqs. (19) and (20) into the total potential energy in Eq. (11) and following the standard FEM procedure, the equilibrium equations of the plate discretized by the ES-MITC3 elements are rewritten as

$$\widehat{\mathbf{K}} \mathbf{d} = \mathbf{F} \quad (21)$$

where  $\widehat{\mathbf{K}}$  is the smoothed global stiffness matrix and assembled from the edge-based smoothed stiffness matrices

$$\widehat{\mathbf{k}}_k = \left( \widehat{\mathbf{B}}_b^k \right)^T \mathbf{D}_b \widehat{\mathbf{B}}_b^k \widehat{A}_k + \left( \widehat{\mathbf{B}}_s^k \right)^T \mathbf{D}_s \widehat{\mathbf{B}}_s^k \widehat{A}_k \quad (22)$$

### 2.3. NS-MITC3 plate element

According to the node-based smoothed FEM [7], strain fields are averaged on domains of elements sharing nodes. These smoothed domains are defined by straight lines connecting the edges’ midpoints with the centroids of node-sharing elements as demonstrated in Fig. 4. As a result, the strain fields in Eqs. (9) and (10) are smoothed on the node-based smoothed domains as follows [11]

$$\begin{Bmatrix} \widetilde{\varepsilon}_x \\ \widetilde{\varepsilon}_y \\ \widetilde{\gamma}_{xy} \end{Bmatrix} = \frac{1}{\widetilde{A}_l} \int_{\widetilde{A}_l} \begin{Bmatrix} \varepsilon_x \\ \varepsilon_y \\ \gamma_{xy} \end{Bmatrix} dA; \quad \begin{Bmatrix} \widetilde{\tau}_{xz} \\ \widetilde{\tau}_{yz} \end{Bmatrix} = \frac{1}{\widetilde{A}_l} \int_{\widetilde{A}_l} \begin{Bmatrix} \tau_{xz} \\ \tau_{yz} \end{Bmatrix} dA \quad (23)$$

where  $\widetilde{A}_l$  is the smoothed domain of node “ $l$ ”.

Substituting the strain – nodal displacement relations in Eqs. (9) and (10) into the Eq. (23), the node-based smoothed strains are rewritten

$$\begin{Bmatrix} \widetilde{\varepsilon}_x \\ \widetilde{\varepsilon}_y \\ \widetilde{\gamma}_{xy} \end{Bmatrix} = \frac{Ez}{1-\nu^2} \begin{bmatrix} 1 & \nu & 0 \\ \nu & 1 & 0 \\ 0 & 0 & (1-\nu)/2 \end{bmatrix} \underbrace{\left[ \frac{1}{\widetilde{A}_l} \sum_{e=1}^{\widetilde{N}_e} \left( \frac{A_e}{3} \sum_{i=1}^3 \mathbf{B}_{bi}^e \mathbf{d}_{ei} \right) \right]}_{\widetilde{\mathbf{B}}_b \mathbf{d}^l} \quad (24)$$

$$\begin{Bmatrix} \bar{\tau}_{xz} \\ \bar{\tau}_{yz} \end{Bmatrix} = \frac{E}{2(1-\nu)} \underbrace{\frac{1}{\bar{A}_l} \sum_{e=1}^{\bar{N}_e} \left( \frac{A_e}{3} \sum_{i=1}^3 \mathbf{B}_{si}^{MITC3,e} \mathbf{d}_{ei} \right)}_{\bar{\mathbf{B}}_s \mathbf{d}^l} \quad (25)$$

in which  $\bar{A}_l$  is the area of node-based smoothed domain “ $l$ ”;  $\bar{N}_e$  and  $d^l$  are respectively number of elements and the nodal displacements belonging to the smoothed domain “ $l$ ”; and  $\bar{\mathbf{B}}_b, \bar{\mathbf{B}}_s$  are the gradient matrices of the in-plane and transverse shear smoothed strains, respectively.

Similarly, using the expressions of the nodal smoothed strains in Eqs. (24) and (25) for the strain energy in the total potential energy in Eq. (11) and following the standard FEM procedure, the discretized equilibrium equations of the plate simulated by the NS-MITC3 elements can be obtained

$$\bar{\mathbf{K}} \mathbf{d} = \mathbf{F} \quad (26)$$

where  $\bar{\mathbf{K}}$  is the smoothed global stiffness matrix and assembled from the node-based smoothed stiffness matrices

$$\bar{\mathbf{k}}_l = \left( \bar{\mathbf{B}}_b^l \right)^T \mathbf{D}_b \bar{\mathbf{B}}_b^l \bar{A}_l + \left( \bar{\mathbf{B}}_s^l \right)^T \mathbf{D}_s \bar{\mathbf{B}}_s^l \bar{A}_l \quad (27)$$

#### 2.4. ES+NS-MITC3 plate element

In the approach of combining the ES- and NS-FEM, the strain fields of the MITC3 plate element are now smoothed on a portion of the edge-based smoothed domains and the other of the node-based smoothed ones as illustrated in Fig. 5(b). To build the smoothed domains including the ES- and NS-ones, each element’s edge  $ed$  is divided into 3 segments as in Fig. 5(b) with the ratio

$$L_1^{ed} = L_3^{ed} = \beta \frac{L^{ed}}{2}; \quad L_2^{ed} = (1 - \beta) L^{ed} \quad (28)$$

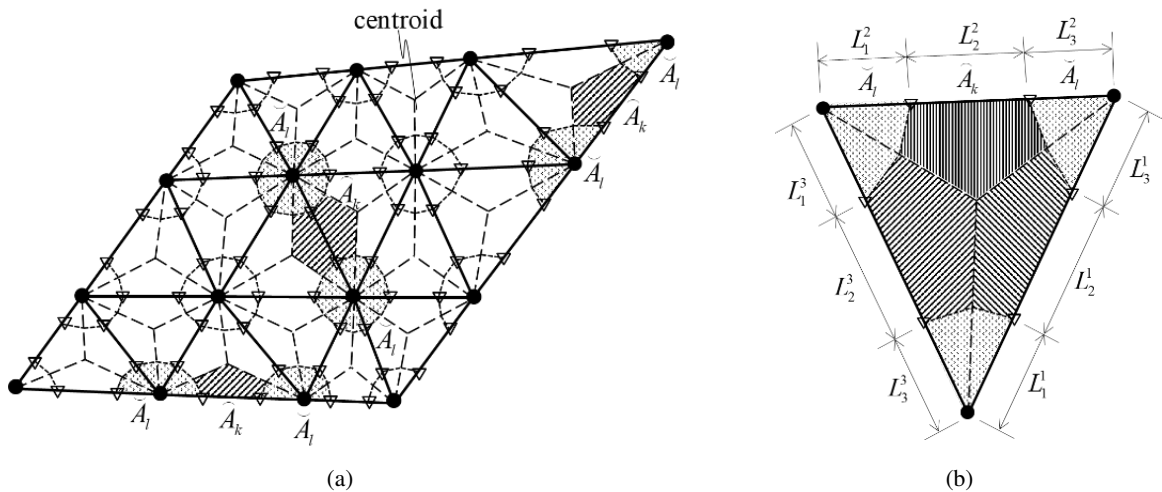


Figure 5. (a) Edge and node-based smoothed domains for a plate discretized by 3-node elements; (b) Definition of the ES- (line hatching) and the NS- (dot hatching) smoothed areas of a triangular element

where  $L^{ed} = L_1^{ed} + L_2^{ed} + L_3^{ed}$ ;  $\beta \in [0, 1]$  is a scale factor used to tune the contribution of the node-based smoothed domains in the ES+NS-domains. It means that if  $\beta = 0$ , the ES+NS-domains become the ES-domains, and if  $\beta = 1$ , the ES+NS-domains are purely NS-ones. This approach is also called the  $\beta$ FEM [12, 13].

From the middle segments  $L_2^{ed}$  and the end segments  $L_1^{ed}$  and  $L_3^{ed}$ , the ES-domains and NS-domains are respectively constructed for elements having common edges and nodes to have the smoothed areas of

$$\hat{A}_k = \beta^2 \hat{A}_k; \tilde{A}_l = (1 - \beta^2) \tilde{A}_l \quad (29)$$

Consequently, the strain fields in Eqs. (9) and (10) averaged on the ES+NS-domains are determined by

$$\begin{Bmatrix} \hat{\varepsilon}_x \\ \hat{\varepsilon}_y \\ \hat{\gamma}_{xy} \end{Bmatrix} = \frac{1}{\hat{A}_k} \int_{\hat{A}_k} \begin{Bmatrix} \varepsilon_x \\ \varepsilon_y \\ \gamma_{xy} \end{Bmatrix} dA; \begin{Bmatrix} \hat{\tau}_{xz} \\ \hat{\tau}_{yz} \end{Bmatrix} = \frac{1}{\hat{A}_k} \int_{\hat{A}_k} \begin{Bmatrix} \tau_{xz} \\ \tau_{yz} \end{Bmatrix} dA \quad (30)$$

$$\begin{Bmatrix} \tilde{\varepsilon}_x \\ \tilde{\varepsilon}_y \\ \tilde{\gamma}_{xy} \end{Bmatrix} = \frac{1}{\tilde{A}_l} \int_{\tilde{A}_l} \begin{Bmatrix} \varepsilon_x \\ \varepsilon_y \\ \gamma_{xy} \end{Bmatrix} dA; \begin{Bmatrix} \tilde{\tau}_{xz} \\ \tilde{\tau}_{yz} \end{Bmatrix} = \frac{1}{\tilde{A}_l} \int_{\tilde{A}_l} \begin{Bmatrix} \tau_{xz} \\ \tau_{yz} \end{Bmatrix} dA \quad (31)$$

Using Eq. (29) and substituting Eqs. (9), (10) into Eqs. (30), (31), the relationships between ES- and NS-strain fields and the nodal displacements in the ES+NS-MITC3 plate element can be derived

$$\begin{Bmatrix} \hat{\varepsilon}_x \\ \hat{\varepsilon}_y \\ \hat{\gamma}_{xy} \end{Bmatrix} = \frac{Ez}{1 - \nu^2} \begin{bmatrix} 1 & \nu & 0 \\ \nu & 1 & 0 \\ 0 & 0 & (1 - \nu)/2 \end{bmatrix} \underbrace{\frac{1}{\beta^2 \hat{A}_k} \sum_{e=1}^{\hat{N}_e} \left( \beta^2 \frac{A_e}{3} \sum_{i=1}^3 \mathbf{B}_{bi}^e \mathbf{d}_{ei} \right)}_{\hat{\mathbf{B}}_b^k} \quad (32)$$

$$\begin{Bmatrix} \hat{\tau}_{xz} \\ \hat{\tau}_{yz} \end{Bmatrix} = \frac{E}{2(1 - \nu)} \underbrace{\frac{1}{\beta^2 \hat{A}_k} \sum_{e=1}^{\hat{N}_e} \left( \beta^2 \frac{A_e}{3} \sum_{i=1}^3 \mathbf{B}_{si}^{MITC3,e} \mathbf{d}_{ei} \right)}_{\hat{\mathbf{B}}_s^k} \quad (33)$$

$$\begin{Bmatrix} \tilde{\varepsilon}_x \\ \tilde{\varepsilon}_y \\ \tilde{\gamma}_{xy} \end{Bmatrix} = \frac{Ez}{1 - \nu^2} \begin{bmatrix} 1 & \nu & 0 \\ \nu & 1 & 0 \\ 0 & 0 & (1 - \nu)/2 \end{bmatrix} \underbrace{\frac{1}{(1 - \beta^2) \tilde{A}_l} \sum_{e=1}^{\tilde{N}_e} \left( (1 - \beta^2) \frac{A_e}{3} \sum_{i=1}^3 \mathbf{B}_{bi}^e \mathbf{d}_{ei} \right)}_{\tilde{\mathbf{B}}_b^l} \quad (34)$$

$$\begin{Bmatrix} \tilde{\tau}_{xz} \\ \tilde{\tau}_{yz} \end{Bmatrix} = \frac{E}{2(1 - \nu)} \underbrace{\frac{1}{(1 - \beta^2) \tilde{A}_l} \sum_{e=1}^{\tilde{N}_e} \left( (1 - \beta^2) \frac{A_e}{3} \sum_{i=1}^3 \mathbf{B}_{si}^{MITC3,e} \mathbf{d}_{ei} \right)}_{\tilde{\mathbf{B}}_s^l} \quad (35)$$

And then, from the total potential energy expressed in the smoothed strain fields given in Eqs. (32)–(35), the equilibrium equations of the plates discretized by ES+NS-MITC3 elements can be written

$$\mathbf{K}^{ES+NS} \mathbf{d} = \mathbf{F} \quad (36)$$

where  $\mathbf{K}^{ES+NS}$  is the edge- and node-based smoothed global stiffness matrix and assembled from the smoothed stiffness matrices

$$\hat{\mathbf{k}}_k = \left(\hat{\mathbf{B}}_b^k\right)^T \mathbf{D}_b \hat{\mathbf{B}}_b^k \hat{A}_k + \left(\hat{\mathbf{B}}_s^k\right)^T \mathbf{D}_s \hat{\mathbf{B}}_s^k \hat{A}_k = \beta^2 \hat{\mathbf{k}}_k \tag{37}$$

$$\tilde{\mathbf{k}}_l = \left(\tilde{\mathbf{B}}_b^l\right)^T \mathbf{D}_b \tilde{\mathbf{B}}_b^l \tilde{A}_l + \left(\tilde{\mathbf{B}}_s^l\right)^T \mathbf{D}_s \tilde{\mathbf{B}}_s^l \tilde{A}_l = (1 - \beta^2) \tilde{\mathbf{k}}_l \tag{38}$$

### 3. Numerical examples

In this section, the accuracy and convergence of the ES+NS-MITC3 element will be evaluated via the patch test and some benchmark plate problems. The results provided by the ES+NS-MITC3 element are compared with similar kinds of elements like ES-DSG3 [8], MITC3 [6], ES-MITC3 [10] and NS-MITC3 [11]. In all the examples, we choose the scale factor  $\beta = 0.6$ . To compare with references, the deflection and moments at the plate center are normalized by

$$\bar{w}_c = w_c \frac{100D}{qL^4}; \quad \bar{M}_c = M_c \frac{10}{qL^2} \tag{39}$$

#### 3.1. Patch test

Consider a patch test be a 0.01 m-thick rectangular plate with the dimension of 0.24 m  $\times$  0.12 m, the Young's modulus  $E = 107 \text{ kN/m}^2$  and the Poisson's ratio  $\nu = 0.25$ . The plate is discretized by 3-node triangular elements as in Fig. 6 [8]. With the deflection equation of the plate  $w = (1 + x + 2y + x^2 + xy + y^2)/200 \text{ m}$ , the ES+NS-MITC3 element can reproduce the deflection and moments at node 5 as shown in Table 1. It means that the ES+NS-MITC3 plate element passes the patch test.

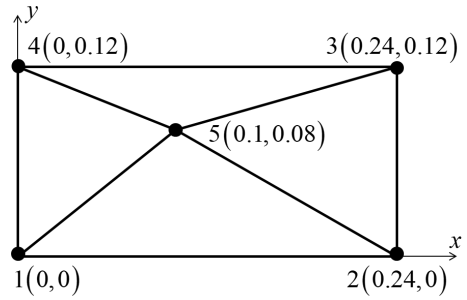


Figure 6. Nodal coordinates of elements discretized for the patch test

Table 1. Deflection and moments of the patch test at node 5

Methods	$w_5 (\times 10^{-2} \text{ m})$	$\theta_{x5} (\times 10^{-2} \text{ rad.})$	$\theta_{y5} (\times 10^{-2} \text{ rad.})$	$M_{x5} (\text{kNm/m})$	$M_{y5} (\text{kNm/m})$	$M_{xy5} (\text{kNm/m})$
ES+NS-MITC3+	0.6422	1.1300	-0.6400	-0.0111	-0.0111	-0.0033
Exact solution	0.6422	1.1300	-0.6400	-0.0111	-0.0111	-0.0033

#### 3.2. Simply supported plate under uniform distributed loading

A square plate of the length  $L$  and the thickness  $h$  is simply supported on the boundary and subjected to the uniform loading  $q = 1 \text{ kN/m}^2$  as illustrated in Fig. 7. The material properties are  $E = 1092000 \text{ kN/m}^2$  and  $\nu = 0.3$ . The plate is modelled by  $2 \times N \times N$  triangular elements in which  $N$  is number of elements on each edge.

The accuracy and convergence of the ES+NS-MITC3 element are studied for the thin plate with the ratio  $h/L = 0.001$  and the thick one with  $h/L = 0.1$ , and the meshes of  $N = 4, 8, 12,$  and  $16$ .

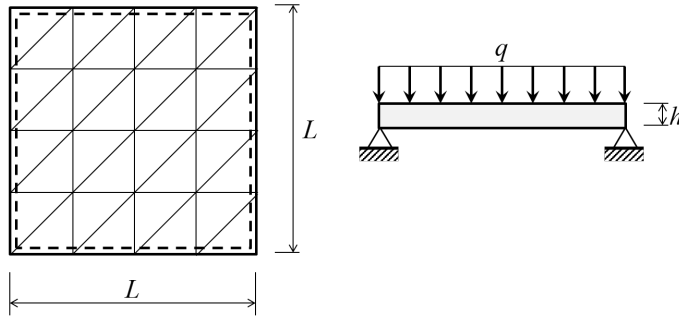


Figure 7. Square plate simply supported on all edges and subjected to uniform distributed loading, and regularly meshed by  $N = 4$  on each plate's edge

The normalized deflections at the plate center provided by the ES+NS-MITC3 element for the ratio  $h/L = 0.001$  and  $h/L = 0.1$  are demonstrated in Fig. 8. In both cases of the plate thickness, the convergence curve given by the ES+NS-MITC3 element lies between those of the ES-MITC3 and NS-MITC3 elements. Therefore, the deflection of the ES+NS-MITC3 element approaches to the analytical solution [16] more rapidly than those of the ES-MITC3 and NS-MITC3 elements. However, the proposed combination of the ES- and NS-domains does not improve the results of moments as illustrated in Fig. 9.

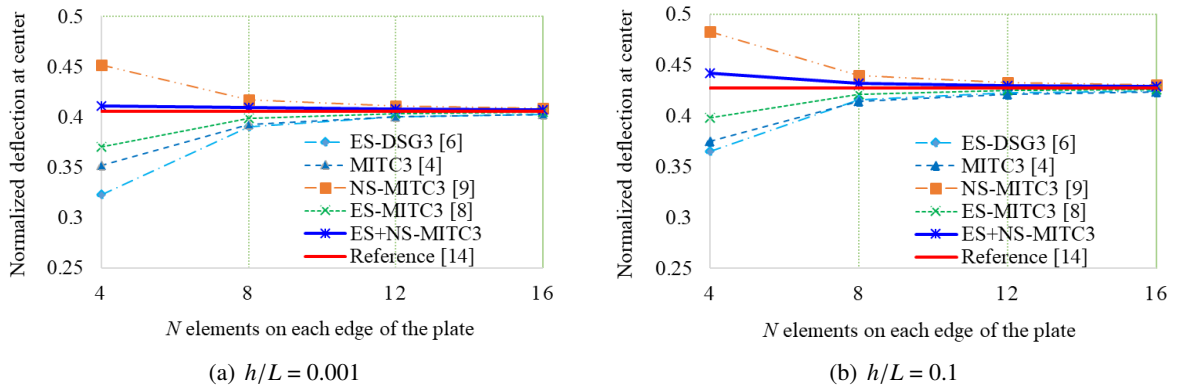


Figure 8. Convergence of the normalized deflections at the center of the simply supported plates under uniform distributed loading

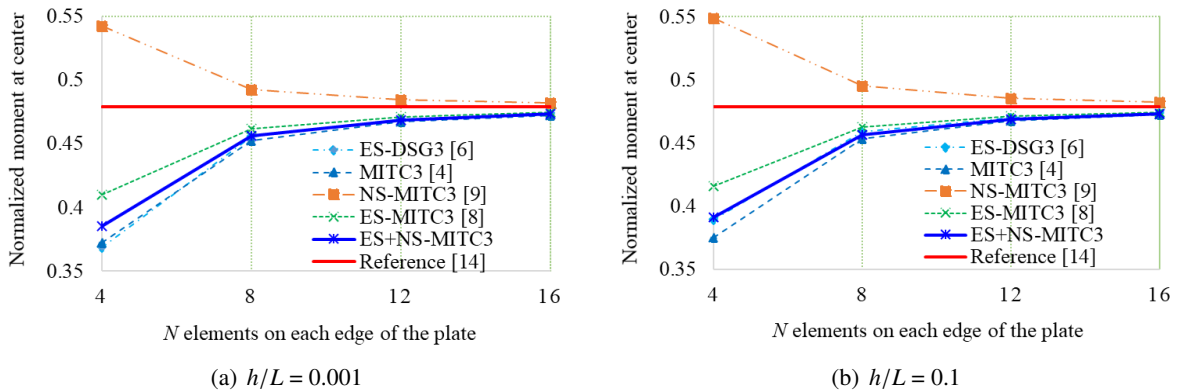


Figure 9. Convergence of the normalized moments at the center of the simply supported plates under uniform distributed loading

### 3.3. Simply supported Morley plate subjected to uniform distributed loading

Consider the rhombus Morley plate [17] of the length  $L = 100$  cm and the thickness  $h = 1$  cm as shown in Fig. 10. The plate is simply supported on all the edges and subjected uniform distributed loading  $q = 0.1$  N/cm<sup>2</sup>. The Young's modulus  $E$  is 109200 N/cm<sup>2</sup> and the Poisson's ratio  $\nu$  is 0.3.

The Morley plate is discretized by different meshes of  $N = 4, 8, 12,$  and  $16$ , in which  $N$  is the number of elements on each edge of the plate (Fig. 10). The normalized deflections and moments at the plate center provided by the proposed element and the other reference ones are compared in Fig. 11 and Fig. 12, respectively. As shown in these figures, the results of the ES+NS-MITC3 element are average values of those given by the ES-MITC3 and NS-MITC3 elements. The deflection of the ES+NS-MITC3 element well converge to the reference solution [17]. However, the accuracy and convergence of the moment given by the ES+NS-MITC3 are not good due to the bad results provide by the NS-MITC3 element. In this case, we can tune the scale factor  $\beta$  to be nearly equal 1.0 to dramatically reduce the overly soft behavior of the node-based smoothed approach.

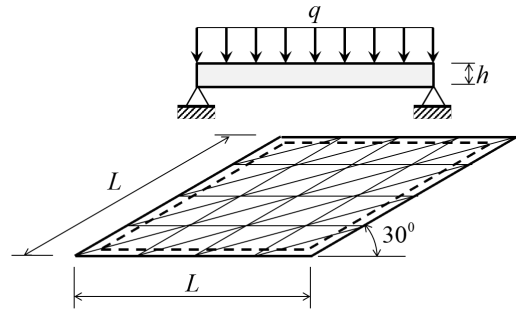


Figure 10. Geometry, uniform distributed loading, and simply supported boundary of the Morley plate with a mesh of  $N = 4$

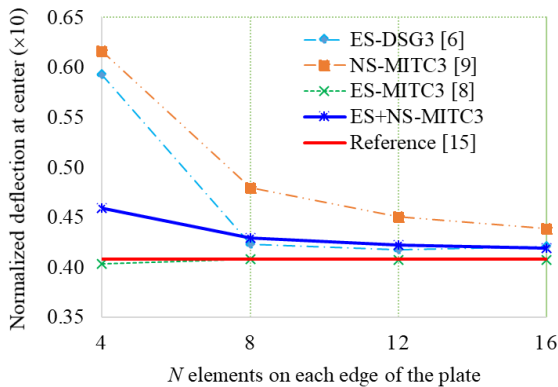


Figure 11. Convergence of the normalized deflections at the center of the Morley plate

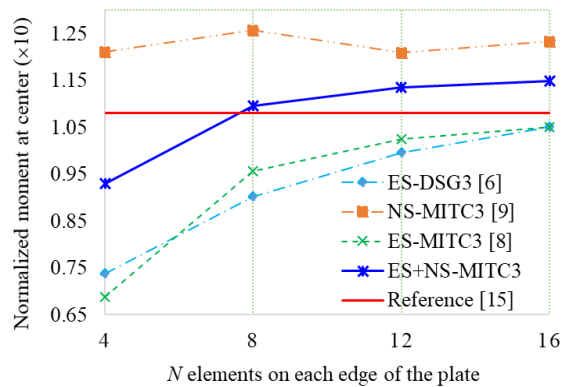


Figure 12. Convergence of the normalized moments at the center of the Morley plate

### 3.4. Clamped circular plate under uniform distributed loading

Give a circular plate with the radius  $R = 5$  m clamped on its circumference and subjected to uniform distributed loading  $q = 1$  kN/m<sup>2</sup> as shown Fig. 13(a). The plate thickness  $h$  with the ratio  $h/R = 0.02$  and  $h/R = 0.2$  are studied. The isotropic homogeneous material of the plate has  $E = 1092000$  kN/m<sup>2</sup>,  $\nu = 0.3$ .

Due to symmetry, a quarter of the plate is meshed by 6, 24, 54 or 96 elements as shown in Fig. 13(b). The deflections and moments at the plate center solved by the ES+NS-MITC3 and other reference elements are respectively demonstrated in Fig. 14 and Fig. 15. Numerical results show that the hybrid model of the ES+NS-MITC3 element can reduce the overly soft behaviors of the NS-MITC3 element and the overly stiff behaviors of the ES-MITC3 to rapidly approach the reference solutions [1] for both thin ( $h/R = 0.02$ ) and thick ( $h/R = 0.2$ ) plates.

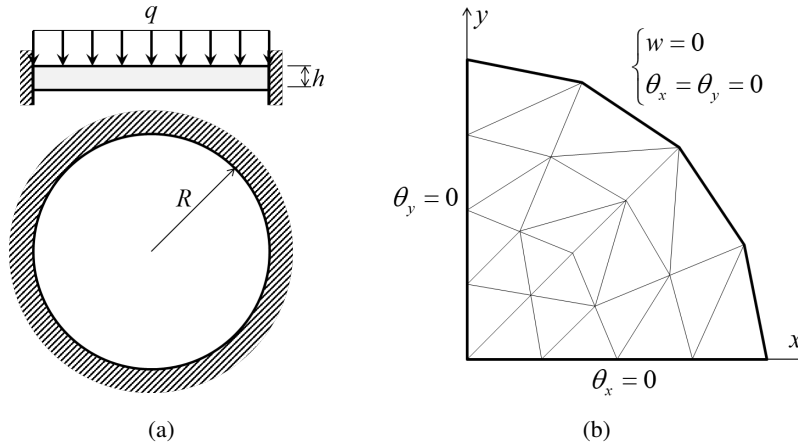


Figure 13. (a) Geometry and loading of the clamped circular plate; (b) A quarter of the plate discretized by 24 triangular elements and symmetric boundaries

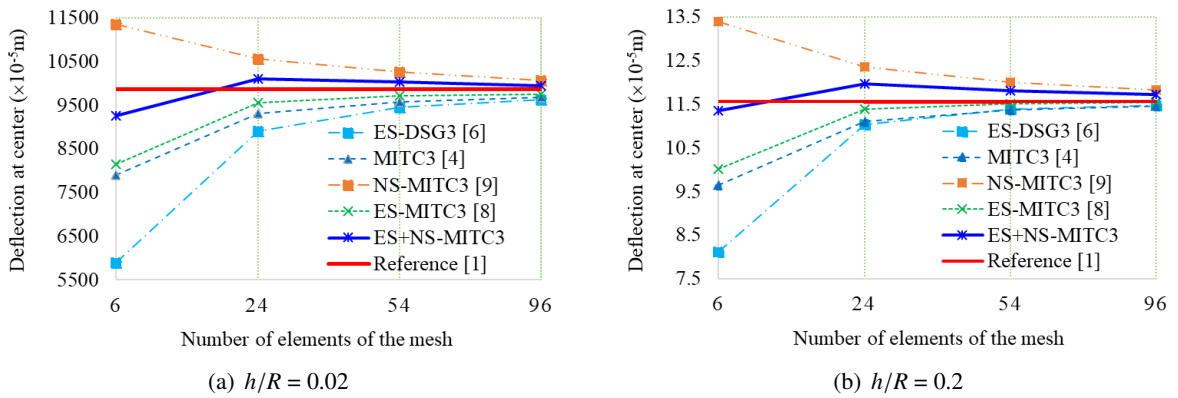


Figure 14. Deflections at the center of the clamped circular plate corresponding to different meshes of 6, 24, 54 and 96 elements

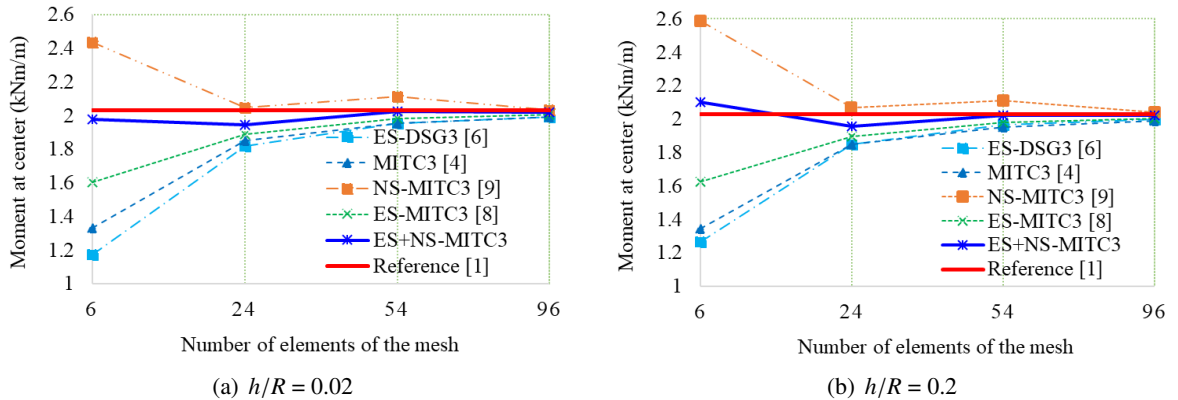


Figure 15. Moments at the center of the clamped circular plate corresponding to different meshes of 6, 24, 54 and 96 elements

#### 4. Conclusions

The  $\beta$ FEM, which is the hybrid approach of the edge-based and node-based smoothed strains, has been developed for the 3-node triangular MITC3 plate elements. The suggested ES+NS-MITC3

element passes the patch test and attenuates the shear-locking phenomenon. The static analyses of some benchmark plate problems show that the ES+NS-MITC3 element can reduce the overly stiff and soft behaviors of the purely ES-MITC3 and NS-MITC3 elements respectively. As a result, the ES+NS-MITC3 element improves the accuracy of the plate deflections and moments as compared with the ES-MITC3 and NS-MITC3 elements, especially in the cases of coarse meshes.

## Acknowledgements

This research is funded by Vietnam National Foundation for Science and Technology Development (NAFOSTED) under grant number 107.02-2017.304.

## References

- [1] Timoshenko, S. P., Woinowsky-Krieger, S. (1959). *Theory of plates and shells*. McGraw-hill.
- [2] Hai, L. T., Tu, T. M., Huynh, L. X. (2018). [Vibration analysis of porous material plate using the first-order shear deformation theory](#). *Journal of Science and Technology in Civil Engineering (STCE) -NUCE*, 12(7):9–19.
- [3] T, T. M., Quoc, T. H., Tham, V. V. (2018). [Analytical solutions for the static analysis of laminated composite plates with piezoelectric layers based on Reddy's higher-order shear deformation theory](#). *Journal of Science and Technology in Civil Engineering (STCE) - NUCE*, 12(4):40–50.
- [4] Tessler, A., Hughes, T. J. R. (1985). [A three-node Mindlin plate element with improved transverse shear](#). *Computer Methods in Applied Mechanics and Engineering*, 50(1):71–101.
- [5] Bletzinger, K.-U., Bischoff, M., Ramm, E. (2000). [A unified approach for shear-locking-free triangular and rectangular shell finite elements](#). *Computers & Structures*, 75(3):321–334.
- [6] Lee, P.-S., Bathe, K.-J. (2004). [Development of MITC isotropic triangular shell finite elements](#). *Computers & Structures*, 82(11-12):945–962.
- [7] Liu, G. R., Nguyen-Thoi, T. (2016). *Smoothed finite element methods*. CRC Press.
- [8] Nguyen-Xuan, H., Liu, G. R., Thai-Hoang, C., Nguyen-Thoi, T. (2010). [An edge-based smoothed finite element method \(ES-FEM\) with stabilized discrete shear gap technique for analysis of Reissner–Mindlin plates](#). *Computer Methods in Applied Mechanics and Engineering*, 199(9-12):471–489.
- [9] Nguyen-Xuan, H., Rabczuk, T., Nguyen-Thanh, N., Nguyen-Thoi, T., Bordas, S. (2010). [A node-based smoothed finite element method with stabilized discrete shear gap technique for analysis of Reissner–Mindlin plates](#). *Computational Mechanics*, 46(5):679–701.
- [10] Chau-Dinh, T., Nguyen-Duy, Q., Nguyen-Xuan, H. (2017). [Improvement on MITC3 plate finite element using edge-based strain smoothing enhancement for plate analysis](#). *Acta Mechanica*, 228(6):2141–2163.
- [11] Chau-Dinh, T., Nguyen-Van, D. (2016). Static and frequency analysis of laminated composite plates using the MITC3 elements having the strains averaged on node-based domains (NS-MITC3). In *Proceedings of the National Science Conference on "Composite Materials and Structures: Mechanics, Technology and Application"*, 613–620.
- [12] Wu, F., Liu, G. R., Li, G. Y., Cheng, A. G., He, Z. C. (2014). [A new hybrid smoothed FEM for static and free vibration analyses of Reissner–Mindlin Plates](#). *Computational Mechanics*, 54(3):865–890.
- [13] Wu, F., Zeng, W., Yao, L. Y., Hu, M., Chen, Y. J., Li, M. S. (2018). [Smoothing Technique Based Beta FEM \( \$\beta\$  FEM\) for Static and Free Vibration Analyses of Reissner–Mindlin Plates](#). *International Journal of Computational Methods*, page 1845006.
- [14] Logan, D. L. (2011). *A first course in the finite element method*. Thomson.
- [15] Lyly, M., Stenberg, R., Vihinen, T. (1993). [A stable bilinear element for the Reissner–Mindlin plate model](#). *Computer Methods in Applied Mechanics and Engineering*, 110(3-4):343–357.
- [16] Taylor, R. L., Auricchio, F. (1993). [Linked interpolation for Reissner-Mindlin plate elements: Part II—A simple triangle](#). *International Journal for Numerical Methods in Engineering*, 36(18):3057–3066.
- [17] Morley, L. S. D. (1963). *Skew plates and structures*. Pergamon Press.